Unified multiconductor transmission-line model of multiple-shield multiconductor cables: evaluation of shield connections performances

J-P. Parmantier, I. Junqua, M. Ridel and S. Bertuol
ONERA/DEMR, Université de Toulouse, F-31055 Toulouse - France

Corresponding author: J-P. Parmantier (e-mail: jean-philippe.parmantier@onera.fr).

ABSTRACT This paper presents a unified transmission-line model of a multiple-shield multiconductor cable. This model includes, at the same time, the propagation and the cross-coupling characteristics of the electrical wires and the cable shields. It also includes the electromagnetic characteristics of the shields (in terms of transfer impedance and transfer admittance). It is derived in compliance with the multiconductor-transmission-line theory and can be applied whatever the connection configurations at both shield extremities. Therefore, it makes it possible the modelling of realistic cable shield connection problems ranging from ideal 360° shield connections to simple bonding wires. The paper proposes a physical explanation of the derived per-unit-length matrices. This unified model is also used to define the required conditions for calculating the electromagnetic coupling response of a shielded cable in a two-step approach in which the shield problem and the inner shield problem are solved in sequence. Finally, the paper illustrates an application of the model in order to evaluate the performances of a shielded cable link on electromagnetic crosstalk configurations with respect to several electrical bonding solutions of the shield.

INDEX TERMS Shielded cables, Transfer impedance, Transfer admittance, Transmission-Lines, Multiconductor-Transmission-Lines, Electromagnetic Compatibility, EMC.

I. INTRODUCTION

Shielded cables are classically used in all Electrical Wiring Interconnected Systems (EWIS) of the industry sector to reduce electromagnetic (EM) radiated and conducted emissions generated by signals flowing on electrical wires and to protect them from EM external sources. In Electromagnetic Compatibility (EMC) applications, transfer-impedance and transfer-admittance (generally called "Z_t" and "Y_t") theoretical concepts are classically used to characterize intrinsic EM performances of shielded cables [1]. The measurement and theoretical evaluation of these cable shield parameters are the subjects of numerous references ([2]-[5]). By the way, some experimental methods are recommended today by the International Electrotechnical Commission (IEC) ([2], [4]) and discussed as IEEE Standards.

Under some specific conditions, modelling and simulation of the EM coupling on a single-shield cable can be performed in two steps that are independently and successively solved. Nevertheless, this "two-step" approach assumes that the currents on the cable shield are much larger than the currents on the electrical wires. Such a property implies specific cable shield installation and bonding conditions at the extremities. In the first step of this approach, the current, I_{ext}, and the voltage, V_{ext}, induced by EM sources are determined on the shield. The computation can be done with a Transmission-Line (TL) model when the shield geometry complies with quasi Transverse-EM (TEM) conditions. However, in the general case, any method, for example a full-wave 3D solver, can be used to obtain the response of the shield. The resulting induced currents along the electrical wires inside the shield, I_{int}, and voltage, V_{int}, are evaluated in the second step of the approach. This time, a TL model is fully appropriate, considering the cable internal geometry. The mathematical link between both steps is made through the induced per unit length (p.u.l) distributed equivalent sources applied on the inner TL model (voltage generators $Z_t.I_{ext}$ and current generators $Y_t.I_{ext}$). The effectiveness of the two-step approach has been validated for a long time. As an example, in [6], its robustness has been experimentally demonstrated to predict the EM coupling onto a complex wiring installed in a Boeing 707 test-bed aircraft submitted to an EM illumination.

In real systems, the performance of cable shields with respect to frequency intimately depends on the quality of their electrical connections to the ground at their extremities. In the case of imperfect connections, it is well known that the two-step approach as explained above may not be correct anymore. However, the theoretical conditions of applicability of the

two-step approach still deserve to be established. For instance, the cross-coupling between the shield and the electrical wires may indeed lead to a possible reaction of the inner wire currents onto the shield currents, which is entirely neglected in the two-step approach.

To overcome the possible limitations of the two-step model, the objective of this paper is to propose a general Multiconductor-Transmission-Line (MTL) model of multiple-shield bundles. We will call this model, the "unified" model. This model is fully consistent because:

- It is rigorously valid for both EM emission and EM susceptibility problems
- It provides the material to derive the theoretical conditions of application of the two-step approach
- It does not depend on the shield electrical connections to the ground
- It does not depend on the number of shields or shield layers (since the shield may be included in each other).

Such a unified model has been implemented and applied at ONERA since 1996 in the CRIPTE computer code [7]. ONERA has developed this code for more than 25 years to evaluate EM interferences on MTL cable networks [6]. It is based on EM topology concepts and solves the wave form of the Baum-Liù-Tesche (BLT) equation on MTL Network (MTLN) models, in the frequency domain [8]. Numerous examples of applications of the CRIPTE code can be found in the literature ([9]-[13]).

The theoretical derivation of the unified model has been published in French references ([14], [15]). The model has also been experimentally validated. In [14], it is used to accurately predict EM fields emitted by a coaxial cable with respect to various configurations of the shield connections to the ground. In [16], the measurement of various types of shielded cables in a triaxial cell is simulated to solve an inverse problem that provides a very large frequency band evaluation of the shield transfer impedance. In [17] and [18], the model is used to simulate complex aeronautical wirings containing different types of shielded cables; comparisons between measurement and calculation responses are provided respectively for S-parameter evaluations between wires and EM-field illumination responses of the electrical wiring.

Unfortunately, as far as we know, the unified model has never been published in such details as in [14] and [15] in an English-written reference. This is why, on the one hand, from section II to IV, this paper provides a detailed reminder of the method as presented in [14] and [15]. In section II, we describe the derivation of the unified model formalism with all major mathematical steps, taking as example a simple coaxial cable. Section III gives a physical interpretation of the resulting unified model p.u.l TL-parameters. The extension to the general model to multiple cable shields and multiple electrical wires is presented in section IV.

On the other hand, sections V and VI provide new material from [14] and [15]. Section V uses the unified model to derive analytically the theoretical conditions for which the classical two-step approach can be legitimately applied. This section specifically illustrates the impact of those assumptions on a test configuration reported in a recent reference ([5]). Section VI demonstrates, in an electrical wiring design process, the capability of the unified model to evaluate finely the impact of the quality of cable shield electrical bonding solutions on the EM-shielding performance. Section VII concludes on the relevance of the two-step and unified model approaches.

II. SINGLE SHIELD LAYER: APPLICATION TO A COAXIAL CABLE

A. TWO-REFERENCE MTL MODEL

As a first step, we illustrate the approach with a simple shielded cable geometry: a one-conductor single shield cable and, more specifically, a coaxial cable. The cable is supposed installed at a constant height, h, over an infinite-dimension ground plane, as presented in Fig.1.

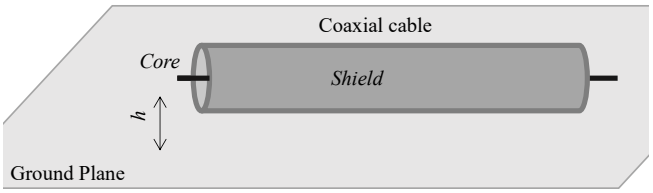

FIGURE 1. Coaxial cable configuration

The entire problem can be decomposed into two TL models. The exterior domain defines the exterior-TL (Fig.2.a); the shield plays the role of the TL signal conductor and the ground plane is the TL return conductor. The interior domain defines the interior-TL (Fig.2.b); the inner core plays the role of the TL signal conductor and the cable shield is the TL return conductor.

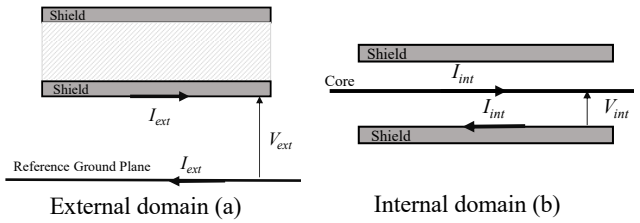

FIGURE 2. Coaxial cable: exterior (left) and interior (right) TL linear-sections of the external domain and internal domain problems

On the one hand, approximating the internal domain by a TL model is straightforward since it can be assimilated to a waveguide structure propagating quasi-TEM modes over a large frequency band. On the other hand, the external domain geometry is equivalent to the usual configuration of a wire over a ground plane, acting as an open waveguide for which the relevance of the TL approximation depends on the geometrical parameters (especially height over the ground plane, length and diameter of the shield) versus frequency. Therefore, the upper frequency limit of the validity of the

exterior TL model is smaller than the frequency limit of the interior-TL model. The outer shield geometry with respect to the ground will always provide the upper frequency limit of the unified model. Nevertheless, assuming the validity of the TL model for the exterior domain, it is possible to write two systems of two equations:

$$\begin{cases} -\frac{dV_{int}}{dz} = Z_{int}.I_{int} - Z_t.I_{ext} \\ -\frac{dI_{int}}{dz} = Y_{int}.V_{int} + Y_t.V_{ext} \end{cases} \quad (1)$$

$$\begin{cases} -\frac{dV_{ext}}{dz} = Z_{ext}.I_{ext} - Z_t.I_{int} \\ -\frac{dI_{ext}}{dz} = Y_{ext}.V_{ext} + Y_t.V_{int} \end{cases} \quad (2)$$

We observe that (1) and (2) mathematically put together:

- The TL p.u.l. impedances (Z_{ext} and Z_{int}) and admittances (Y_{ext} and Y_{int}) together with the cable-shield transfer impedance and transfer admittance Z_t and Y_t
- The currents and voltages of the external domain (I_{ext} and V_{ext}) and the currents and voltages of the internal domain (I_{int} and V_{int})

We call this model the "two-reference" model because the voltages have two different references (the ground plane for the exterior-TL and the shield for the interior-TL). For this purpose, an external current and an internal current, flowing on both sides of the shield, are defined, implicitly assuming that the shield has a non-zero thickness.

In both (1) and (2) systems of equations, the transfer parameters appear as reciprocal terms providing the cross-coupling between both the external and internal domains. This formulation enables the simulation of either EM-emission or EM-susceptibility configurations with the same model. Putting together voltages and currents in vectors in (1) and (2), the two vector equations of the two-reference TL model of this two-conductor TL (the shield arbitrarily being the first conductor and the inner core, the second conductor) are obtained:

$$-\frac{d}{dz}\begin{pmatrix} V_{ext} \\ V_{int} \end{pmatrix} = [Z_{2ref}].\begin{pmatrix} I_{ext} \\ I_{int} \end{pmatrix} \quad (3)$$

$$-\frac{d}{dz}\begin{pmatrix} I_{ext} \\ I_{int} \end{pmatrix} = [Y_{2ref}].\begin{pmatrix} V_{ext} \\ Y_{int} \end{pmatrix} \quad (4)$$

in which $[Z_{2ref}]$ and $[Y_{2ref}]$ are the 2x2 p.u.l. impedance and admittance matrices of the equivalent two-reference MTL model of the coaxial cable, the two conductors of the MTL being the shield and the inner core:

$$[Z_{2ref}] = \begin{bmatrix} Z_{ext} & -Z_t \\ -Z_t & Z_{int} \end{bmatrix} \quad (5)$$

$$[Y_{2ref}] = \begin{bmatrix} Y_{ext} & Y_t \\ Y_t & Y_{int} \end{bmatrix} \quad (6)$$

B. SINGLE-REFERENCE MTL MODEL

As far as EMC applications are concerned, there is a usual need to refer all voltages to a common reference in order to be able to comply with common-mode measurements and all common mode related issues. To this extent, equations (1) and (2) have to be expressed with respect to a single ground reference. For this purpose, we still consider our coaxial cable problem as a 2-conductor TL but, this time, both conductors are referenced to the ground plane. The shield is still the first conductor and the inner core still the second conductor. From this perspective, the voltages $V_{i(i=1,2)}$ and currents $I_{i(i=1,2)}$ defined for this single-reference model, as schemed in Fig.3, can be mathematically related to the voltages and the currents of the two-reference model:

$$\begin{cases} V_1 = V_{ext} \\ I_1 = I_{ext} - I_{int} \\ V_2 = V_{ext} + V_{int} \\ I_2 = I_{int} \end{cases} \quad (7)$$

The V_2 voltage, defined as the voltage between the reference ground plane and the core, is the sum of voltage between the ground plane and the shield (V_{ext}) and the voltage between the shield and the core (V_{int}).

Moreover, the total current on the shield, I_1, is the sum of the shield currents flowing externally (I_{ext}) and internally (I_{int}) in opposite directions.

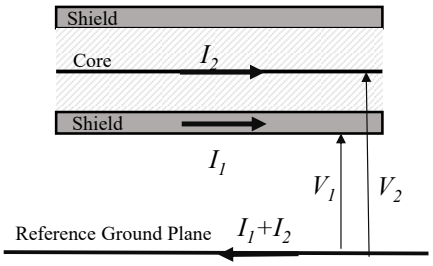

FIGURE 3. Coaxial cable: single-reference TL-model

Introducing (7) in equations (3) and (4) leads to the two equations of the single-reference two-conductor TL model, now referenced to the ground plane. The new expressions of the p.u.l impedance and admittance matrices of the TL (referenced to the ground plane) write:

$$[Z_{1ref}] = \begin{bmatrix} Z_{ext} & Z_{ext} - Z_t \\ Z_{ext} - Z_t & Z_{int} + Z_{ext} - 2.Z_t \end{bmatrix} \quad (8)$$

$$[Y_{1ref}] = \begin{bmatrix} Y_{int} + Y_{ext} - 2.Y_t & Y_t - Y_{int} \\ Y_t - Y_{int} & Y_{int} \end{bmatrix} \quad (9)$$

III. PHYSICAL SIGNIFICANCE OF p.u.l. PARAMETERS

Equations (5) and (6) as well as (8) and (9) show that the Z_t and Y_t parameters can be considered as MTL parameters. Moreover, the formulation of p.u.l impedance and admittance matrices (8) and (9) entirely summarizes in a compact way the overall shielding properties of shielded cables. In this section, we want to show that such a MTL formulation entirely

complies with other well-known knowledge or provides useful information on the way the transfer parameters affect the EM shielding mechanisms of shielding cables. For this purpose, we take again the example of the coaxial cable.

A. P.U.L. DC RESISTANCE MATRIX

From (8), the p.u.l. DC-resistance matrix $[R_{1ref}]$, value of the p.u.l. impedance matrix at $f=0$ (or limit of its real part when f goes to 0), can be expressed as a function of the p.u.l. DC-internal-resistance, R_{int}, the DC-external-resistance, R_{ext} and the DC-transfer-resistance of the shield, R_t, as:

$$[R_{1ref}] = \begin{bmatrix} R_{ext} & R_{ext} - R_t \\ R_{ext} - R_t & R_{int} + R_{ext} - 2.R_t \end{bmatrix} \quad (10)$$

Let us now suppose a 1m-long coaxial cable with both the core and the shield short-circuited to the ground at the right hand side to force the total current to return in the ground plane as expected in our single-reference model. At $f=0$, we can derive a pure resistive equivalent electrical circuit scheme as in Fig.4, in which we introduce the DC-resistances of each equivalent conductor of the system:

- R_g, the p.u.l DC resistance of the ground plane,
- R_s, the p.u.l DC resistance of the shield,
- R_c, the p.u.l DC resistance of the core.

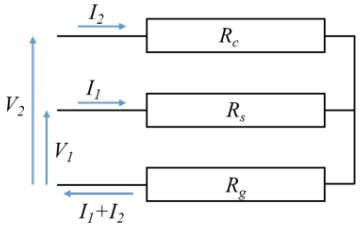

FIGURE 4. Equivalent resistive electrical circuit model of the 1m-long short-circuited coaxial cable problem

$V_{i(i=1,2)}$ and $I_{i(i=1,2)}$ are the TL voltages and currents as defined in the single-reference MTL model. The circuit can be seen from the left hand side as a two-port system. The DC relationship between voltages and currents of this circuit network writes:

$$\begin{bmatrix} V_1 \\ V_2 \end{bmatrix} = \begin{bmatrix} R_s + R_g & R_g \\ R_g & R_c + R_g \end{bmatrix} \cdot \begin{bmatrix} I_1 \\ I_2 \end{bmatrix} \quad (11)$$

and provides another expression of the resulting resistance matrix referenced to the ground plane, $[R_{1ref}]$:

$$[R_{1ref}] = \begin{bmatrix} R_s & 0 \\ 0 & R_c \end{bmatrix} + \begin{bmatrix} R_g & R_g \\ R_g & R_g \end{bmatrix} \quad (12)$$

in which:

- The p.u.l. DC resistance of the reference, R_g appears on the extra-diagonal terms,
- The diagonal terms are the sum of the reference p.u.l. DC-resistance and the p.u.l. DC-resistance of either the shield or the core.

Besides, we can express R_{int} and R_{ext}, the p.u.l DC-resistances of the two-reference MTL model. For the internal-TL, the reference is the shield, so:

$$R_{int} = R_c + R_s \quad (13)$$

For the external-TL, the reference is the ground plane, so:

$$R_{ext} = R_s + R_g \quad (14)$$

Equaling (10) and (12) implies $R_t=R_s$, that is to say, the well-known result that the p.u.l. transfer resistance, R_t, is equal to the DC transfer resistance of the shield, R_s. The DC part of (8) therefore complies with the underlying DC electrical circuit of the MTL.

B. P.U.L. INDUCTANCE MATRIX

In the single-reference model, the p.u.l. inductance matrix $[L_{1ref}]$ is obtained from the high frequency limit of the imaginary part of the p.u.l impedance matrix, $[Z_{1ref}]$, divided by the pulsation, $\omega=2\pi f$. By introducing the internal and external inductance terms, L_{int} and L_{ext}, and the transfer inductance L_t term in (8), the p.u.l. inductance matrix writes:

$$[L_{1ref}] = \begin{bmatrix} L_{11} & L_{12} \\ L_{21} & L_{22} \end{bmatrix} = \begin{bmatrix} L_{ext} & L_{ext} - L_t \\ L_{ext} - L_t & L_{int} + L_{ext} - 2.L_t \end{bmatrix} \quad (15)$$

The p.u.l. inductance matrix can be understood from the definition of each ($L_{ij,(i,j=1,2)}$) term introducing the definition of the p.u.l. magnetic fluxes as:

$$L_{11} = \frac{\Phi_1}{I_1}\Big)_{I_2=0} \text{ and } L_{12} = \frac{\Phi_1}{I_2}\Big)_{I_1=0} \quad (16)$$

$$L_{21} = \frac{\Phi_2}{I_1}\Big)_{I_2=0} \text{ and } L_{22} = \frac{\Phi_2}{I_2}\Big)_{I_1=0} \quad (17)$$

where Φ_1 and Φ_2 are the magnetic fluxes between conductor 1 (conductor 2 respectively), and the reference ground plane (Fig.5). These two fluxes can be decomposed as elementary fluxes:

$$\Phi_1 = \Phi_{ext} - \Phi_{l-int} \quad (18)$$

$$\Phi_2 = \Phi_{ext} - \Phi_{l-int} + \Phi_{int} - \Phi_{l-ext} \quad (19)$$

with:

- $\Phi_{ext} = L_{ext}.I_{ext}$: flux outside the shield,
- $\Phi_{l-int} = L_t.I_{int}$: exterior flux due to internal magnetic field leakages through the shield,
- $\Phi_{int} = L_{int}.I_{int}$: flux inside the shield,
- $\Phi_{l-ext} = L_t.I_{ext}$: interior flux due to external magnetic field leakages through the shield.

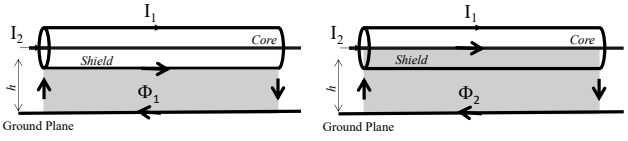

FIGURE 5. Physical significance of Φ_1 and Φ_2 in the single-reference model of the coaxial problem

When no current is flowing in the core ($I_2=0$, $I_1=I_{ext}$ and $I_{int}=0$), there is no leakage outside the shield and the magnetic field inside the shielded-cable is only due to leakage of the external magnetic field. (18) and (19) write as:

$$\Phi_1\rangle_{I_2=0} = \Phi_{ext} = L_{ext}.I_1 = L_{11}.I_1 \quad (20)$$

$$\Phi_2\rangle_{I_2=0} = L_{ext}.I_1 - L_t.I_1 = L_{21}.I_1 \quad (21)$$

When no current is flowing in the shield ($I_1=0$, $I_2=I_{int}$), the current flowing on the core ($I_2=I_{int}$) is equal to the current I_{ext}. These two currents ($I_{int}=I_{ext}$), generate simultaneously intrinsic fluxes and leakage fluxes in the internal and in the external domains. Then (18) and (19) write as:

$$\Phi_1\rangle_{I1=0} = L_{ext}.I_2 - L_t.I_2 = L_{12}.I_2 \quad (22)$$

$$\Phi_2\rangle_{I1=0} = L_{ext}.I_2 - L_t.I_2 + L_{int}.I_2 - L_t.I_2 = L_{22}.I_2 \quad (23)$$

The magnetic field based equations, (16) to (23), verify the single-reference MTL inductance matrix model (15). The transfer inductance, L_t, characterizes the leakage of the magnetic field through the shield. Besides, when the shield is ideal (no L_t), the remarkable inductance property of shielded cables, $L_{11}=L_{12}$, is also verified.

C. P.U.L. CAPACITANCE MATRIX

In the single-reference model, the p.u.l. capacitance matrix $[C_{1ref}]$ is obtained from the high frequency limit of the imaginary part of all terms of the p.u.l. admittance matrix, $[Y_{1ref}]$, divided by $\omega=2\pi f$. By introducing the internal and external p.u.l. capacitance terms, C_{int} and C_{ext}, and the p.u.l. transfer capacitance, C_t, in (9), the p.u.l capacitance matrix writes:

$$[C_{1ref}] = \begin{bmatrix} C_{11} & C_{12} \\ C_{21} & C_{22} \end{bmatrix} = \begin{bmatrix} C_{int} + C_{ext} - 2.C_t & C_t - C_{int} \\ C_t - C_{int} & C_{int} \end{bmatrix} \quad (24)$$

C_{ext} represents the p.u.l. capacitance between the shield and the reference plane and C_{int}, the p.u.l capacitance between the core and the shield.

Similarly as done for the resistance matrix assessment, we consider a 1m-long cable. We leave this time both conductors of the coaxial TL-equivalent problem of the right hand side in open circuit, as described in Fig. 6. As for a usual two-port system seen from the left hand side of the TL, the circuit can be modelled as an equivalent capacitance network with an "effective" equivalent capacitances C^e_{ij}, placed between each pair of conductors i and j.

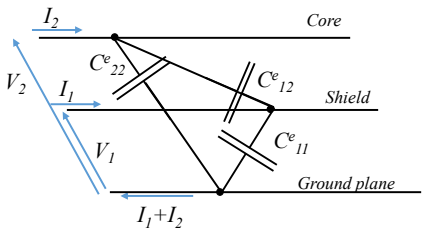

FIGURE 6. Equivalent circuit model of the 1m-long open-circuited coaxial cable problem

The resolution of Fig.6 circuit network provides the following matrix relationship between the voltages and the currents:

$$\begin{bmatrix} I_1 \\ I_2 \end{bmatrix} = j\omega \begin{bmatrix} C^e_{12} + C^e_{11} & -C^e_{12} \\ -C^e_{12} & C^e_{12} + C^e_{22} \end{bmatrix} . \begin{bmatrix} V_1 \\ V_2 \end{bmatrix} \quad (25)$$

Equaling the terms of (24) and (25), the p.u.l. transfer capacitance, C_t, appears as an effective capacitance directly connecting the core and the reference ground plane. It represents the leakages of the electric field through the shield. Because of these leakages, the p.u.l. effective capacitances are equal to the initial C_{ext} and C_{int} minus the p.u.l transfer capacitance C_t. Finally the cross-section circuit of the coaxial cable over the ground plane can be summarized under Fig.7's circuit capacitance network model.

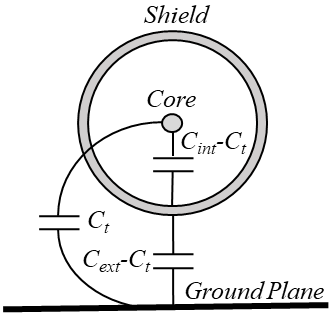

FIGURE 7. Effective capacitance model of the coaxial cable over a ground plane

IV. GENERALIZATION OF THE UNIFIED MODEL TO SEVERAL SHIELD LEVEL MULTICONDUCTOR CABLES

A. ONE-SHIELDING LEVEL MULTICONDUCTOR CABLE

Several multiconductor shielded cables (one shielding level only, i.e. no other shields are included inside the cable shields) are now considered. In this case, the previous example of the coaxial cable can be easily generalized to multiconductor cables by replacing all scalar parameters by matrices and vectors in the systems of equations (1) and (2). Therefore, still having only one shield level, it is possible to consider N_s shielded cables with N_w internal conductors; (3) and (4) relationships remain the same. To obtain the multiple reference model extended to MTLs, we can first gather all the shield equivalent wires for having an exterior-MTL, referenced to the ground plane, and characterized by $N_s \times N_s$ $[Z_{ext}]$ and $[Y_{ext}]$ p.u.l. impedance and admittance matrices. Second, we can gather the N_w interior-MTLs p.u.l. impedance and admittance matrices referenced to their own cable-shield, building thereby two large $[Z_{int}]$ and $[Y_{int}]$ p.u.l. impedance and admittance matrices. The p.u.l. impedance matrix, $[Z_{Mref}]$ and p.u.l admittance matrix $[Y_{Mref}]$ of the multiple-references models are then obtained by concatenating the interior and exterior MTL matrices as previously done for the coaxial cable

problem. Then $[Z_{Mref}]$ and $[Y_{Mref}]$ synthetize the whole MTL model and are organized in 4 sub-blocks as follows:

$$[Z_{Mref}] = \begin{bmatrix} [Z_{ext}] & -[Z_t] \\ -[Z_t] & [Z_{int}] \end{bmatrix} \quad (26)$$

$$[Y_{Mref}] = \begin{bmatrix} [Y_{ext}] & [Y_t] \\ [Y_t] & [Y_{int}] \end{bmatrix} \quad (27)$$

where $[Z_{ext}]$ (or $[Y_{ext}]$) and $[Z_{int}]$ (or $[Y_{int}]$) respectively appear in the diagonal upper and lower blocks. The off-diagonal blocks $[Z_t]$ and $[Y_t]$ represent the cross-coupling between the external domain and the internal domains. They contain the transfer impedance and admittance terms of each of the N_s shields.

The associated single-reference unified model can be easily obtained by applying a base transformation, defined as a generalization of the scalar relationships in (7), between the voltage and current vectors in the multiple-reference system, $[V_{Mref}]$, $[I_{Mref}]$, and the voltage and current vectors in the single-reference system, $[V_{1ref}]$ and $[I_{1ref}]$. This transformation involves $[P_v]$ and $[P_i]$, normed passing matrices relating those vectors, for voltages and currents respectively. We have:

$$[I_{1ref}] = [P_i].[I_{Mref}] \quad (28)$$

$$[V_{1ref}] = [P_v].[V_{Mref}] \quad (29)$$

Since those matrices are real (filled with "0", "1" and "-1" terms) and normed, the inverse of the passing matrices for voltages and currents can be obtained from their transposed matrices as:

$$[P_v]^{-1} = [P_i]^T \quad (30)$$

$$[P_i]^{-1} = [P_v]^T \quad (31)$$

If we introduce (28) to (31) into (3) and (4), we can write the single-reference p.u.l. impedance and admittance matrices as a function of the $[Z_{Mref}]$ and $Y_{Mref}]$ p.u.l. impedance and admittance matrices:

$$[Z_{1ref}] = [P_v].[Z_{Mref}].[P_i]^T \quad (32)$$

$$[Y_{1ref}] = [P_i].[Y_{Mref}].[P_v]^T \quad (33)$$

B. GENERALIZATION TO SEVERAL SHIELD LEVELS

Relations (32) and (33) have been derived for a single cable shield level only. Now, the process is extended to several shield levels (when shields are included into other shields). The derivation of the unified MTL model can be obtained from an iterative process consisting in the following steps:

- Decomposition of the problem in cable shield levels (CSL_i),
- Ordering of the shield levels from the smallest to the largest: CSL_1, CSL_2, … CSL_i, CSL_{i+1}…, the smallest index being the deepest in terms of inclusion of shields,
- Generation of the i^{th} MTL model at each CSL_i,
- For each pair $\{CSL_i, CSL_{i+1}\}$, application of the single reference model and repetition of this model by climbing up to the upper CSL_k.

Such an iterative process can be done step-by-step or in a global explicit formulation. As a final result, equations (32) and (33) still apply but the passing matrices, $[P_v]$ and $[P_i]$ are transformed accordingly to the *CSL* ordering.

C. EXAMPLE

In order to illustrate how the one-reference p.u.l. impedance and admittance matrices, $[Z_{1ref}]$ and $[Y_{1ref}]$ are built, we consider the example schemed in Fig.8. It consists of two coaxial cables over a ground plane. The two shields are named *S1* and *S2*: their respective internal cores are named *C1* and *C2*.

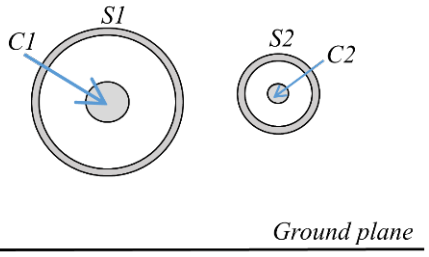

FIGURE 8. Example of two coaxial cables in parallel to a ground plane (geometrical cross-section)

The unified model is made of four equivalent wires that are ordered as follows: {*S1, S2, C1, C2*}. The two-reference p.u.l. impedance matrix $[Z_{Mref}]$ can be written as in (26):

$$[Z_{Mref}] = \begin{bmatrix} Z_{S1,S1} & Z_{S1,S2} & -Z_{t1} & 0 \\ Z_{S2,S1} & Z_{S2,S2} & 0 & -Z_{t2} \\ -Z_{t1} & 0 & Z_{int1} & 0 \\ 0 & -Z_{t2} & 0 & Z_{int2} \end{bmatrix} \quad (34)$$

Where:

- Z_{t1} and Z_{t2} are the p.u.l. transfer impedances of the 2 coaxial cables,
- Z_{int1} and Z_{int2} are the p.u.l. internal domain impedances of the cores *C1* and *C2*, of the two coaxial cables, referenced to the *S1* and *S2* shields,
- $\begin{bmatrix} Z_{S1,S1} & Z_{S1,S2} \\ Z_{S2,S1} & Z_{S2,S1} \end{bmatrix}$ is the p.u.l. impedance block matrix of the external-domain MTL, constituted by the two shields *S1* and *S2*, with respect to the ground plane.

Note that the associated p.u.l. admittance matrix $[Y_{Mref}]$ has the same structure; the only difference is that the terms $-Z_{ti}$ are replaced by $+Y_{ti}$.

The passing matrices, $[P_v]'$ and $[P_i]'$, write as follows (before normalization):

$$[P_v]' = \begin{bmatrix} 1 & 0 & 0 & 0 \\ 0 & 1 & 0 & 0 \\ 1 & 0 & 1 & 0 \\ 0 & 1 & 0 & 1 \end{bmatrix} \quad (35)$$

$$[P_i]' = \begin{bmatrix} 1 & 0 & -1 & 0 \\ 0 & 1 & 0 & -1 \\ 0 & 0 & 1 & 0 \\ 0 & 0 & 0 & 1 \end{bmatrix} \quad (36)$$

The last step consists in applying (32) and (33) in order to obtain the one-reference p.u.l. impedance and admittance matrices, $[Z_{1ref}]$ and $[Y_{1ref}]$. We obtain:

$$[Z_{1ref}] = \begin{bmatrix} Z_{S1,S1} & Z_{S1,S2} & Z_{S1,S1} - Z_{t1} & Z_{S1,S2} \\ Z_{S2,S1} & Z_{S2,S2} & Z_{S1,S2} & Z_{S2,S2} - Z_{t2} \\ Z_{S1,S1} - Z_{t1} & Z_{S2,S1} & Z_{S1,S1} - 2Z_{t1} + Z_{int1} & Z_{S1,S2} \\ Z_{S2,S1} & Z_{S2,S2} - Z_{t2} & Z_{S2,S1} & Z_{S2,S2} - 2Z_{t2} + Z_{int2} \end{bmatrix} \quad (37)$$

$$[Y_{1ref}] = \begin{bmatrix} Y_{S1,S1} - 2Y_{t1} + Y_{int1} & Y_{S1,S2} & Y_{t1} - Y_{int1} & 0 \\ Y_{S2,S1} & Y_{S2,S2} - 2Y_{t2} + Y_{int2} & 0 & Y_{t2} - Y_{int2} \\ Y_{t1} - Y_{int1} & 0 & Y_{int1} & 0 \\ 0 & Y_{t2} - Y_{int2} & 0 & Y_{int2} \end{bmatrix} \quad (38)$$

V. CONDITIONS OF APPLICABILITY OF THE TWO-STEP APPROACH

As mentioned in the introduction, the widespread way to compute induced currents/voltages response on internal conductors of shielded cables consists in the two-step approach, which is legitimate under specific assumptions only (see Section I). Since the unified model of multiconductor shielded cables is general, we will use it in the following to validate theoretically the domain of applicability of this two-step approach. In what follows, we will address only sources induced from Z_t since the sources coming from Y_t can be generally neglected compared to the sources coming from Z_t. We will then illustrate this domain of applicability by an example.

A. THEORETICAL DERIVATIONS

Let us consider the one-conductor single shield cable problem in Fig.9, similar to the one in Fig.1. We have introduced the current and voltage notations of the single-reference unified model.

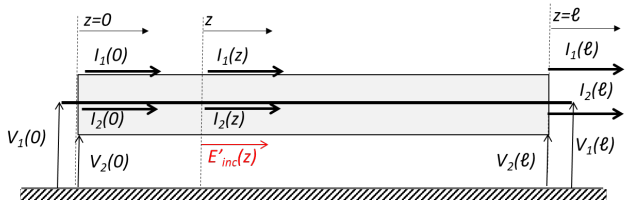

FIGURE 9. One-conductor shielded cable used for the derivation of the two-steps approach application domain

The length of the cable is ℓ. $[I(z)]$ and $[V(z)]$ are respectively the current and voltage vectors at a position z along the cable. Both vectors are constituted of the currents $I_1(z)$, $I_2(z)$ on the one hand and the voltages $V_1(z)$, $V_2(z)$ on the other hand, respectively on both the shield and the core TL-equivalent wires:

$$[I(z)] = \begin{bmatrix} I_1(z) \\ I_2(z) \end{bmatrix} \text{ and } [V(z)] = \begin{bmatrix} V_1(z) \\ V_2(z) \end{bmatrix} \quad (39)$$

The currents and voltages respectively take the values $I_1(0)$, $I_2(0)$, $V_1(0)$, $V_2(0)$ at the origin of the TL, $z=0$ (left hand side), and $I_1(\ell)$, $I_2(\ell)$, $V_1(\ell)$, $V_2(\ell)$ at the remote end of the TL, $z=\ell$, (right hand side).

To have a general derivation of the solution, we consider that the cable is illuminated by an incident EM field (i.e. a field in the absence of the cable) which tangential component along the cable is $E'_{inc}(z)$. Referring to Agrawal's Field-to-Transmission-Line (FTL) model ([10], [15], [19]), this distributed tangential component is equal to the distributed voltage generators induced on all equivalent wires of the MTL model, i.e. on both the shield and the core equivalent wires. If we make the reasonable assumption that both wires are co-localized, those voltage generators are equal on both MTL equivalent wires. Note also that the application of Agrawal's FTL model implies that the voltages $V_i(z)$ are not defined as "total" voltages but "scattered" voltages (derived from the scattered electric field only). However, the currents $I_i(z)$ remain the total currents and this restriction does not change the nature of the conclusions on the model.

Consequently, the first MTL equation writes:

$$\frac{d[V(z)]}{dz} = -[Z].[I(z)] + [E'_{inc}(z)] \quad (40)$$

where $[Z]$ is the p.u.l. impedance of the MTL model as in (8).

The derivation of the two-step approach will be made at low frequency, under the resonance regime of the TL for which all variables can be considered as not influenced by the propagation characteristics of the MTL. We will then see that the conclusions for the conditions of application of the approach can be generalized to the resonant frequency regime of the cable.

Under the low frequency approximation, (40) may then be developed as:

$$\begin{bmatrix} V_1(0) - V_1(\ell) \\ V_2(0) - V_2(\ell) \end{bmatrix} = [Z].\ell.\begin{bmatrix} I_1(\ell) \\ I_2(\ell) \end{bmatrix} - \begin{bmatrix} E_{inc} \\ E_{inc} \end{bmatrix} \quad (41)$$

where the total induced voltage E_{inc} comes from the integration of the distributed generators $E'_{inc}(z)$ over ℓ.

$$E_{inc} = \int_0^{\ell} E'_{inc}(z).dz \quad (42)$$

We now consider specific load conditions at the extremity of the shielded-cable. The shield is short-circuited at both extremities to cope with required installation conditions. The core is short-circuited at position $z=0$ and loaded by an impedance Z_{core} at position $z=\ell$. Fig. 10 represents the electrical model of the shielded-cable in this load configuration that imposes the conditions $V_1(0)=V_1(\ell)=V_2(0)=0$. I_1 and I_2 are the simplified notations for the low frequency approximation currents that can be

supposed constant along ℓ: $I_1=I_1(0)=I_1(\ell)$ and $I_2=I_2(0)=I_2(\ell)$. Thereby, (41) now writes:

$$\begin{bmatrix} 0 \\ -V_2(\ell) \end{bmatrix} = [Z].\ell.\begin{bmatrix} I_1 \\ I_2 \end{bmatrix} - \begin{bmatrix} E_{inc} \\ E_{inc} \end{bmatrix} \tag{43}$$

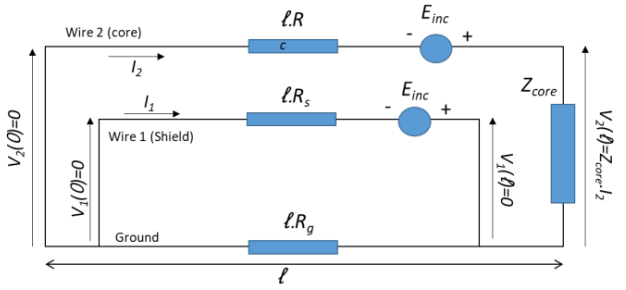

FIGURE 10. Low frequency circuit model of the shielded-cable with specific load configuration

The development of (43), using (8) gives:

$$E_{inc} = Z_{ext}\ell I_1 + (Z_{ext} - Z_t)\ell I_2 \tag{44}$$

$$-Z_{core}I_2 = -Z_t\ell I_1 + (Z_{int} - Z_t)\ell I_2 \tag{45}$$

The two-step approach implies that there is no reaction from the internal current on the core over the current on the shield. Thereby, the following conditions must be fulfilled from (44):

$$\|Z_{ext}I_1\| \gg \|(Z_{ext} - Z_t)I_2\| \tag{46}$$

From (45) we may write:

$$I_2 = \frac{Z_t\ell I_1}{Z_{core}+(Z_{int}-Z_t)\ell} \tag{47}$$

The combination of (46) and (47) provides the general condition on the various impedances involved in the problem to apply the two-step approach:

$$\left\| Z_{ext}.\left(\frac{Z_{core}}{\ell} + Z_{int} - Z_t\right)\right\| \gg \|(Z_{ext} - Z_t).Z_t\| \tag{48}$$

At DC, using (13), (14) and notations of Fig.10, condition (48) leads to:

$$\left(R_s + R_g\right)\left(\frac{\lim_{DC} Re(Z_{core})}{\ell} + R_c\right) \gg R_gR_s \tag{49}$$

Since $R_s+R_g>R_g$, condition (49) will be verified whatever the value of the ground resistance, R_g if:

$$\left(\frac{\lim_{f\to 0} Re(Z_{core})}{\ell} + R_c\right) \gg R_s \tag{50}$$

(50) now copes with the agreed wiring design practice that the sum of the DC limit of the common-mode end-loads and the total resistance of the core must be much larger that the total resistance of the shield.

At higher frequency (but before the propagation regime), when the inductance contribution to the impedance dominates the resistance, condition (48) for applying the two-step approach can be rewritten as:

$$\boldsymbol{L_{ext}\left(\frac{\lim_{HF} Im(Z_{core})}{\ell} + L_{int} - L_t\right) \gg (L_{ext} - L_t).L_t} \tag{51}$$

Since the transfer inductance of a shielded cable used for EM shielding, L_t, is much lower than the external inductance, L_{ext}, (51) can be simplified by:

$$\boldsymbol{\left(\frac{\lim_{HF} Im(Z_{core})}{\ell} + L_{int}\right) \gg 2L_t} \tag{52}$$

At high frequency, condition (52) implies that the total equivalent inductance of the inner TL must be much larger than two times the total transfer inductance of the shield. This condition generally makes the two-step approach valid at high frequency as well, even in the resonance region, provided that the current on the shield is correctly estimated.

B. TWO-STEP APPROACH TL MODELS

Under the condition (46), (44) becomes:

$$E_{inc} = Z_{ext}\ell I_1 \tag{53}$$

which means that the calculation of the shield current at the first step can be made with the model of the exterior TL alone excited by the incident field equivalent generators.

However, (45) deserves to be derived independently at DC and HF limits in order to identify the appropriate TL model of the second step. We respectively find:

$$R_tI_1 = \frac{\lim_{f\to 0} Re(Z_{core})}{\ell} I_2 + R_cI_2 \tag{54}$$

and

$$j\omega L_tI_1 = \frac{\lim_{HF} Im(Z_{core})}{j\omega\ell} I_2 + j\omega(L_{int} - L_t)I_2 \approx \frac{\lim_{HF} Im(Z_{core})}{j\omega\ell} I_2 + j\omega L_{int}I_2 \tag{55}$$

On the one hand, at DC, (54) shows that the TL model is based on the resistance of the core, R_c, only (and not on the addition of R_t, the cable shield resistance, as the interior-TL model would have required it). On the other hand, the right hand side of (55) is obtained with the already mentioned reasonable assumption that $L_{int}>>L_t$. In this case, the model involves the interior-TL inductance, L_{int}. Besides, both (54) and (55) indicate that the source term of the second step TL model is equal to $Z_t.I_1$, therefore depending on the current calculated at the first step. With respect to these conclusions, Fig. 11 summarizes the p.u.l. circuit cells of the two TL models to be applied in the two-step approach.

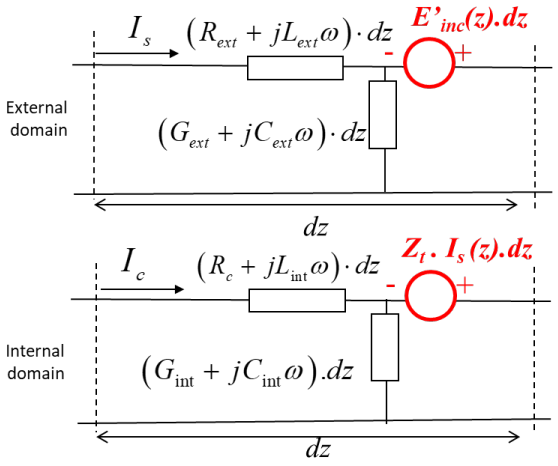

FIGURE 11. The two-step approach TL circuit cell model. Above, TL-cell for the calculation of the shield current I_s. Below, TL-cell for the calculation of the core current I_c.

C. APPLICATION EXAMPLE

As an illustration, we consider the measurement set-up proposed in [5] for measuring the transfer impedance of a RG058 coaxial cable (Fig. 12).

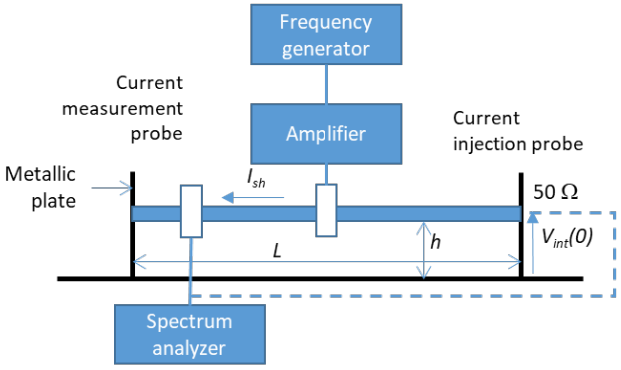

FIGURE 12. Z_t scalar measurement setup applied on a RG058 cable (from [5]).

The shielded cable, of length L, is installed over a perfectly conducting ground, between two metallic plates at a height of h=10cm. The shield ends are perfectly connected to the two plates. The inner conductor is connected to a 50 Ω resistance on the right hand side plate and is short-circuited to the left hand side plate. In this section, the first objective is to validate our unified model by simulating the reference [5] "scalar measurement setup" with the CRIPTE code (see Section I). The principle of the measurement is very classical and obviously based on the two-step approach (the notations are intentionally the same as in [5]):

- The current on the shield, I_{sh}, is injected with a frequency generator driving a current injection probe through an amplifier. I_{sh} is measured with a current measurement probe connected to a spectrum analyzer
- The voltage on the inner conductor, $V_{int}(0)$, is measured with a spectrum analyzer
- The module of the transfer impedance, Z_t, is obtained from the classical formula:

$$Z_t = \frac{V_{int}(0)}{L.I_{sh}} \tag{56}$$

in which L is the length of the cable.

The RG058 cable characteristics provided in [20] are sufficient to derive the one reference MTL model of the cable:

- p.u.l. resistance of the inner core = 39.2 mΩ/m
- p.u.l. capacitance = 100 pF/m
- Characteristic impedance = 50 Ω
- Approximate inner conductor diameter = 0.9 mm
- Approximate insulation (and shield) diameter = 2.95 mm
- Velocity ratio=66%

With respect to [5], the signature of the measured transfer impedance indicates that Z_t can be simplified as:

$$Z_t = R_t + j\omega RL_t, \tag{57}$$

with:

- R_t= 14 mΩ/m
- L_t= 1 nH/m

Such a simplification is hopefully possible here because [5] does not provide any information on the phase of Z_t.

Besides, the authors mention that the "*presence or the absence of the measuring probe during the measurement of $V_{int}(0)$ has no particular influence on the results*". Therefore, we can model the current injection probe as an ideal transformer. For this, we assume that its primary circuit produces an ideal voltage generator E on any secondary wire circuits made by the cables under tests [21] and we can assume no reaction of this secondary circuit on the primary circuit. Since the coaxial cable MTL model is made of two equivalent wires (the inner core and the shield), the voltage generator E must be applied on both wires as shown in Fig. 13 (note the analogy with Agrawal's model in Fig. 10 where the current injector can be seen as a local incident tangential field transducer). Finally, equation (56) being independent of E, we can set it arbitrarily to E=1V in our MTL simulations.

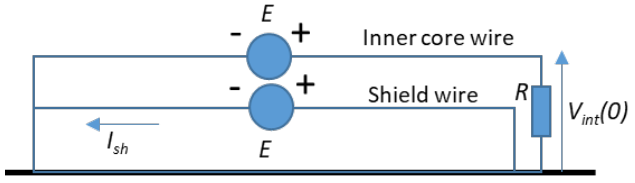

FIGURE 13. Equivalent circuit model of the Z_t scalar measurement setup applied on the RG058 cable (from [5]).

In Fig.14, we show the simulation results of Z_t obtained with the unified model and the classical two-step model. The perfect accordance with [5] validates our unified model. In this measurement configuration, we also verify that the

assumption of the two-step approach, on which the measurement technique is based, is logically fulfilled.

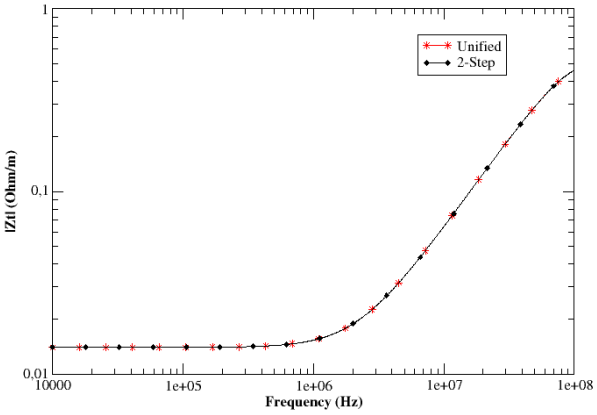

FIGURE 14. Zt simulation with the reference [5] scalar measurement setup. Unified model and two-step approach

In the following, we investigate the second objective of this section: analyze the impact of the conditions of application of the two-step approach. For this, we consider two additional specific test configurations based on Fig.12 for stressing the RG058 cable and we compute $V_{int}(0)$, both with the two-step approach and with the unified model:

- *Configuration B*: the shield is supposed disconnected from the right hand side plate (the connection is supposed having been damaged) and the inner conductor is still connected to R=50 Ω. In this configuration, the assumptions to apply the two-step approach are clearly not satisfied.
- *Configuration C*: the shield is supposed having been damaged, which results in a new transfer resistance value, R_t=40 mΩ/m, and a new transfer inductance value, L_t=2 nH/m. The shield is still supposed ideally grounded at its extremities. However, R, the right-hand side end resistance of the core is now set to a very low value, R=1 mΩ. In this configuration, the resistance of the shield is of the same order of value as the resistance of the core, so we can anticipate that the two-step approach might be defaulting.

The resulting computed voltages on the core, $V_{int}(0)$, are plotted in Fig. 15.

As a reference, the initial ideal configuration A of [5] (shield ideally grounded, core loaded by 50 Ω) labelled by "Conf A" is also plotted. Comparisons between both types of models, two-step and unified, (respectively labelled "2-Step" and "Unified") are consistent with the expectations regarding the conditions of applicability of the two-step approach. In configuration A only, the two-step approach perfectly fits with the unified model approach over the whole frequency range, which explains why the Z_t results are in perfect agreement with [5]. In configuration C (labelled "Conf C"), the two-step approximation provides in average good results but we note a discrepancy in a frequency band for which either the resistance or the inductance dominate. In configuration B (labelled "Conf B"), the two-step condition is not verified due to the disconnection of the shield to the ground and the two models do not match. Note that, in configuration B, since the shield is disconnected, the EM shielding effect is null and, at low frequency, the induced voltage on the core computed by the unified model is, as expected, logically equal to E=1V.

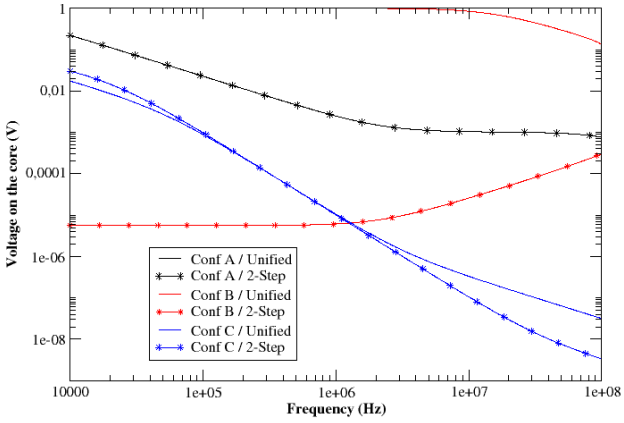

FIGURE 15. Voltage induced on the core $V_{int}(0)$ – Unified and two-step model results of various test setup configurations

VI. EM SHIELDING PERFORMANCE AS A FUNCTION OF THE SHIELD END ELECTRICAL CONNECTIONS

A. OBJECTIVE

The efficiency of a shielded cable link depends on several parameters. Among them, the most significant ones are the shield properties, the shielding effectiveness of connectors, and the electrical connection of the shield to the connector chassis. The objective, here, is to show how the unified single-reference shielded cable model can be used to evaluate the performances of shielded cable links as a function of the nature of the shield connections at the extremities. Assuming the connectors are perfectly grounded, the ideal shield connection is the 360° connection around the surface of the connector in order to extend the shield geometry up to the ground. Very often, due to installation constraints, connector typologies or maintenance requirements, such an ideal electrical connection is not always feasible and has to be replaced by a bonding wire. Sometimes, even worse solution, there are no electrical connections to the ground at the extremities of the shields. Hereafter, we will analyze the EM shielding effectiveness to demonstrate the impact of such shield connections on generic configurations. As in section V-C, the demonstration will be made by numerical MTL simulations performed with the CRIPTE code (see section I) based on the unified model.

B. DESCRIPTION OF THE TEST CASE

As an illustration, we consider the generic test installation illustrated in Fig. 16. Two types of Shielded Test Cables, *STCi* (*STC1* or *STC2*), are installed in turn at a height of h=10 cm

over a ground plane, between two perfectly conducting metallic plates, *P1* and *P2* (shown in transparency in the figure). The distance between *P1* and *P2* is ℓ=1m. We suppose that the ground plane has an equivalent ground resistance, R_g=10 mΩ/m between *P1* and *P2*. A bare wire *W1* is running in parallel to both *STCi* at the same height *h* and at a distance *d*=5 mm. *W1* is short-circuited to the ground and, passing through a hole in *P1,* is connected to the ground with a *R*=50 Ω resistance on the outer face of *P1*. On this outer face of *P1*, a voltage generator *E*=1V is applied to drive a current on *W1* and makes it act as an EM field illuminator on both *STCi*.

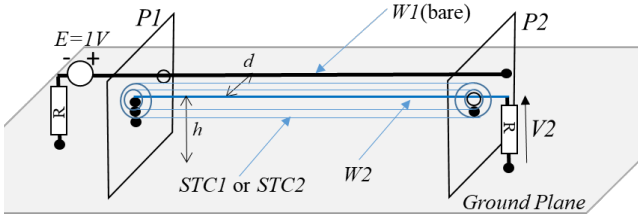

FIGURE 16. Scheme of the Shielded Test Cable installation. The black dots figure perfect connections; the absence of black dots figure the possibility of imperfect connections.

As shown in Fig.17, both *STCi* are made as follows:

- The Shielded Test Cable *STC1* consists of a wire, *W2,* surrounded by a single shield, *S1* (single shield test cable configuration),
- The Shielded Test Cable *STC2* consists of the previous *STC1* surrounded by a second shield *S2* (overshielded test cable configuration).

W2 is short-circuited on *P1* and, passing through a hole in *P2*, is connected with a *R*=50 Ω resistance to the ground on the outer face of *P2*. Both the resistances *R* and the voltage generator *E* are supposed to be infinitely small compared to the 1 m distance between *P1* and *P2*.

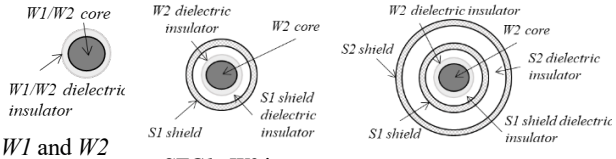

W1 and *W2* alone

STC1: W2 in shielded configuration

STC2: W2 in overshielded configuration

FIGURE 17. Geometrical cross-sections of *W1/W2, STC1 and STC2*

W1 and *W2* are considered to be two identical and parallel wires with the following characteristics:

- Radius of the wires = 0.25 mm
- Radius of the wire dielectric insulators = 0.55 mm
- Relative dielectric permittivity of the dielectric insulators = 2.3
- p.u.l. resistance of the wires = 117.5 mΩ/m

The characteristics of the first shield, *S1*, are:

- Radius of *S1* = 1.1 mm
- Transfer resistance of *S1*: R_t = 70 mΩ/m
- Transfer inductance of *S1*: L_t = 3 nH/m

The characteristics of the second shield, *S2,* are:

- Radius of *S2* = 2.29 mm
- Transfer resistance of *S2*: R_t = 7 mΩ/m,
- Transfer inductance of *S2*: L_t = 4 nH/m
- Relative dielectric permittivity of the medium between *S2* and *S1* = 1.0

Three configurations of shield electrical connections at the extremities are considered for *STC1* and *STC2* (Fig. 18. and Fig. 19):

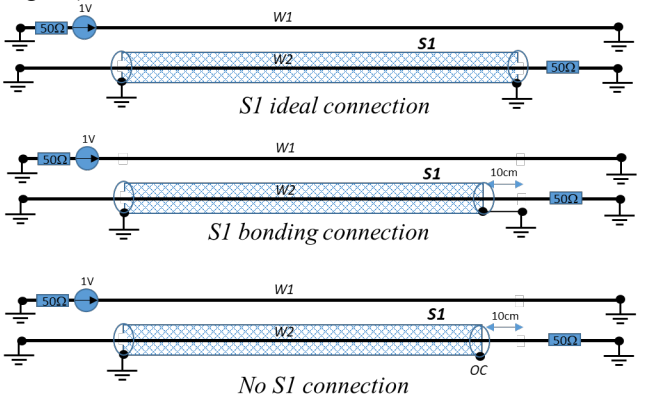

FIGURE 18. Electrical shield connections at the extremities for the Shielded Test Cable *STC1*

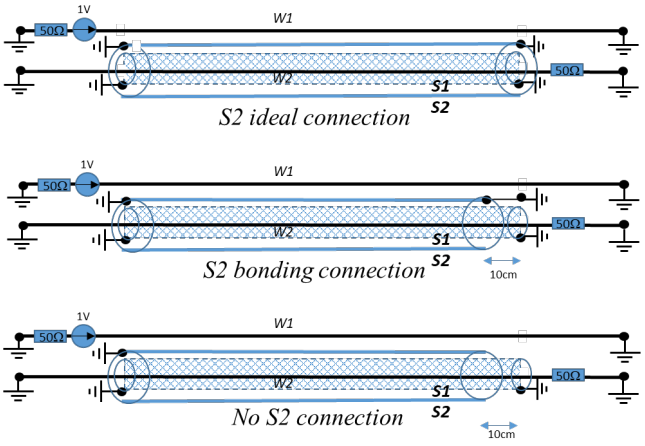

FIGURE 19. Electrical shield connections at the extremities for the Shielded Test Cable *STC2*

- *Ideal end connections:* both extremities of *S1*, for *STC1*, and of *S1* and *S2*, for *STC2*, are ideally short-circuited (360° connection) on *P1* and *P2*.
- *Connection with a bonding wire:* the external shield is 10-cm shortened away from the *P2*-end and connected to the ground via a 10-cm straight bonding wire connected to *P2*. Along this 10-cm distance, the cable is not shielded (for *STC1*) or not overshielded (for *STC2*) anymore. At the opposite extremity (*P1*), the connection is always ideal. For *STC2*, *S1* is supposed to be always ideally short-circuited to *P1* and *P2* at both extremities. The bonding wire being an extension of the external shield, we approximate its p.u.l resistance as the same as the external

shield. Along this 10 cm distance, EM cross-coupling must be considered between *W1*, *W2*, the bonding wire and, eventually, *S1*, in the case of *STC2*.

- *Deteriorated connection:* the external shield is set in open circuit 10 cm away from its far-end extremity at *P2* for both *STC1* and *STC2*. Along this 10-cm distance, *W2* is not shielded or not overshielded anymore. At the opposite extremity the connection is ideal on *P1*.

C. RESULTS

As a first step, V_2 on *W2* is plotted versus the frequency when there is no shield around it at all (Fig. 20). We call it "V_{2ref}". If we remind that *W1* is excited by a voltage generator, the frequency response is typical of a far end crosstalk frequency response with the following signature characteristics:

- At very low frequencies, below about 1 kHz, the voltage is constant with the frequency and is equal to $R_g.\ell/R$,
- When the ground resistance, R_g, becomes negligible compared to the inductance and before frequency resonances (here between 1 kHz and about 50 MHz), the voltage varies linearly with the frequency,
- At higher frequencies, over 50 MHz, a classical frequency resonant signature is observed.

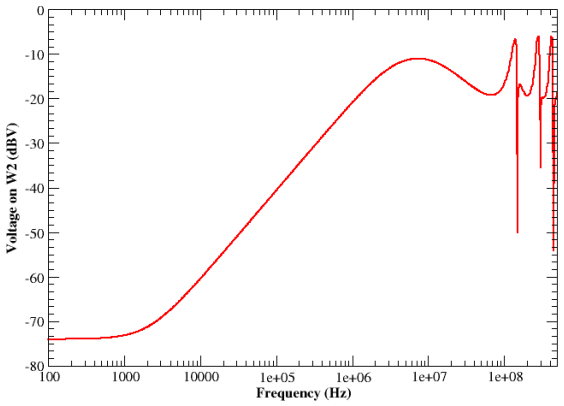

FIGURE 20. Voltage V_{2ref} induced on *W2* (bare wire with no shield at all) – Far end crosstalk

Then, we evaluate the performances of the electrical bonding connections by computing the shielding effectiveness (SE) of the cable link, defined in this case as the ratio between the voltage V_2 on the 50 Ω load of *STC1/STC2* over the voltage V_{2ref} (Fig.21):

$$SE = \frac{V_2}{V_{2\text{ref}}} \tag{58}$$

The SE frequency variations calculated by CRIPTE in all shield end connection configurations are plotted in Fig.21.

These results put to the fore that:

- For the same electrical connection solution of the shield, at low frequencies, the overshield configuration (*STC2*) increases the SE, as expected, by about 10dB up to 30-40 dB in the medium frequency bandwidth.
- For both shielded and overshielded configurations (*STC1* and *STC2*), the 10-cm bonding wire starts degrading the SE from about 100kHz, when the direct cross-coupling between *W1*, the bonding wire, and *W2* starts dominating over the EM coupling on the shielded section.

Finally, we observe that disconnecting an extremity of the external shield significantly damages the SE. In the case of the overshielded configuration (*STC2*), since only the external shield is disconnected at one extremity, the internal shield still brings EM attenuation and the effectiveness becomes similar to the performance of the single shielded configuration (*STC1*).

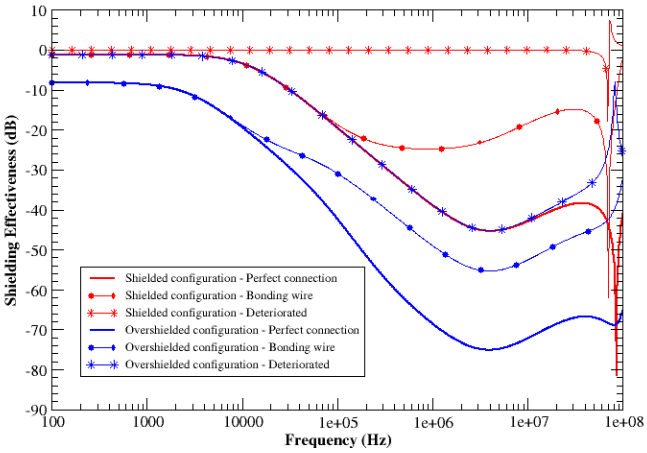

FIGURE 21. Shielding effectiveness for the various electrical shielding solutions of W_2 (CRIPTE calculations)

VII. CONCLUSION

In this paper, we have proposed a MTL model accounting for cables with several shielding levels. This model includes the transfer impedance and admittance of the cable shields in the expressions of the p.u.l impedance and admittance matrices. The model is named "unified model" because it can be applied for any conditions of loads of the shields at the ends of the MTL. In this model, the shields are considered as equivalent wires of the MTL.

When the shields are correctly short-circuited at their extremities and when the shield resistance is lower than the resistance of the cores, this unified model entirely complies with the simplified two-step model in which the equivalent induced p.u.l. voltage generators are proportional to the product of the transfer impedance by the current flowing on the shield. In this paper, we have established the conditions under which the two-step model is applicable. Under these conditions, we have established the two equivalent TL-models to be applied in sequence in the two-step model. Especially, we have shown that a special attention must be paid on the TL-model to be used in the second step for the inner wire response because it slightly differs from the inner TL-problem used to establish the unified model.

From a general modelling perspective, the unified model has the advantage to be general, allowing one to model any type of electrical connection of the MTL shields, without the requirement to have its extremities short-circuited to the ground as required for the classical two-step approach. Finally, even if the illustrations proposed in this paper mainly concern EM coupling, the model has also the advantage to address EM emission problems with as much generality (as shown in [14]). As a conclusion, such a model can be used for the design of cable bundle topologies for which the efficiency of the cable shields cannot be perfect and for which a balance between the installation constraints and the shield characteristic is needed.

REFERENCES

[1] E. Vance, *Coupling to shielded-cables*, Editor : John Wiley & Sons Inc, 1979

[2] *Metallic Communication Cable Test Methods* - Part 4-15: *Electromagnetic Compatibility (EMC) - Test Method for Measuring Transfer Impedance and Screening Attenuation - or Coupling Attenuation With Triaxial Cell*, IEC 62153-4-15:2015, Dec. 4, 2015.

[3] Demoulin and L. Kone, *Shielded-cables transfer impedance measurement,* IEEE EMC Soc. Newslett., vol. 2010, no. 227, pp. 38–45, 2010.

[4] *Metallic Communication Cable Test Methods*: Part 4-6: EMC – *Surface Transfer Impedance - Line Injection Method*, IEC 62153-4-6: 2006, May 9, 2006.

[5] Z. E. Mohamed Chérif, G. Andrieu, G. Alerto, N. Ticaud, C. Julien, *Transfer Impedance Measurement of Shielded-cables Through Localized Injection*, IEEE Trans. Electromagn. Compat., vol. 60, no. 4, pp. 1018-1021, Aug. 2018, DOI: 10.1109/TEMC.2017.2760161.

[6] J. P. Parmantier, F. Issac, I. Junqua & al, *An application of Electromagnetic Topology on the Test Bed Aircraft EMPTAC* Interaction Note 506 – November 1993. available at: http://ece-research.unm.edu/summa/notes/

[7] J. P. Parmantier, S. Bertuol, and I. Junqua*, CRIPTE: Code de réseaux de lignes de transmission multiconducteur*, *User's guide – Version 5.1,* ONERA/DEMR/T-N119/10 - CRIPTE 5.1 2010.

[8] C. E. Baum, T. K. Liù, F. M. Tesche, *On the Analysis of General Multiconductor Transmission-Line Networks*, Interaction Notes, Note 350, November 1978, [Online]. available at: http://ece-research.unm.edu/summa/notes/.

[9] J-P. Parmantier, *Numerical coupling models for complex systems and results*, IEEE Trans. Electromagn. Compat., vol. 46, no. 3, pp. 359-367, Aug. 2004, DOI: 10.1109/TEMC.2004.831818.

[10] L. Paletta, J-P. Parmantier, F. Issac, P. Dumas, J.-C. Alliot, *Susceptibility analysis of wiring in a complex system combining a 3-D solver and a transmission-line network simulation*, IEEE Trans. Electromagn. Compat., vol. 44, no. 2, pp. 309–317, May 2002.

[11] S. Arianos, M. A. Francavilla, M. Righero, F. Vipiana, P. Savi, S. Bertuol, M. Ridel, J-P Parmantier, L. Pisu, M. Bozzetti and G. Vecchi, *Evaluation of the modeling of an EM illumination on an aircraft cable harness,* IEEE Trans. Electromagn. Compat., vol. 56, no. 4, pp. 844–853, Aug 2014.

[12] C. Kasmi, M. Darces and M. Hélier, *Statistical analysis of a spurious signal level in a low voltage PLC network*, International Symposium on Electromagnetic Compatibility - EMC EUROPE, 2012, pp. 1-5, DOI: 10.1109/EMC Europe. 2012.6396777

[13] X. Ferrières, J-P. Parmantier, S. Bertuol, A. Ruddle, *Application of hybrid finite difference / finite volume to solve an automotive problem*, IEEE Trans. Electromagn. Compat., vol. 46, no 4, pp. 624–634, Nov. 2004

[14] J-P. Parmantier, F. Issac, S. Bertuol, F. Boulay : *Modèle unifié d'un câble multiconducteur blindé : application à la susceptibilité et à l'émission électromagnétique* - CEM 2000 Clermont-Ferrand. 14/16 mars 2000, pp 131-136

[15] P. Degauque et J-P. Parmantier, Chapitre 2 : *Couplage aux structures filaires*, in *Compatibilité Electromagnétique*, Collection technique et scientifique des télécommunications, Lavoisier, Hermes. Paris 2007. In French

[16] S. Bertuol, J-P. Parmantier, F. Issac, I. Junqua, P. Foutrel, *Cellule triaxiale à discontinuité de blindage pour la caractérisation de câbles blindés élémentaires par une approche combinée de mesures et de calculs*, CEM 2006 Saint-Malo. 4/6 April 2006,

[17] M. Ridel, P. Savy, J.-P. Parmantier, *Characterization of Complex Aeronautic Harness – Numerical and Experimental Validations*". IEEE Trans. Electromagn. Compat. - Volume 33 – Issue 5 – 2013 pp.341-352 – 2013

[18] S. Arianos, M. A. Francavilla, M. Righero, F. Vipiana, P. Savi, S. Bertuol, M. Ridel, J-P. Parmantier, L. Pisu, M. Bozzetti, G. Vecchi, *Evaluation of the Modeling of an EM Illumination on an Aircraft Cable Harness*. IEEE Transactions on EMC, Vol. 26, 4, Aug. 2014, pp. 844-853

[19] F.M. Tesche, M.V. Ianoz, T. Karlsson, "*EMC Analysis Methods and Computational Models*", John Wiley & Sons, pp.247–266. 1997

[20] *RG58 Coaxial Cable*, Farnell data sheet. [Online] Available at: https://www.farnell.com/datasheets/2095749.pdf

[21] J.P. Parmantier, *S-parameter determination with a pair of current injection and measurement probes*. Interaction Notes. Note 552. October 1998. [Online] Available at: http://ece-research.unm.edu/summa/notes/.